DOI: 10.1021/cg9008637

CRYSTAL GROWTH & DESIGN Article

2010, Vol. 10
232–236

Morphology Evolution of Cu_2O from Octahedra to Hollow Structures

Yuebin Cao, Junmei Fan, Liuyang Bai, Fangli Yuan,* and Yunfa Chen

State Key Laboratory of Multi-phase Complex System, Institute of Process Engineering, Chinese Academy of Sciences, Beijing 100190, P. R. China, and Graduate University of the Chinese Academy of Sciences, Beijing 100049, P. R. China

Received July 24, 2009; Revised Manuscript Received October 11, 2009

ABSTRACT: Octahedral Cu_2O crystals with an edge length about 1 μm were synthesized by reducing a copper-citrate complex with glucose. The morphology and structure of Cu_2O particles were greatly affected by the concentration of glucose, reaction temperature, and time. When the concentration of glucose increased from 0.6 to 1.6 M, the morphology of Cu_2O could be changed from octahedral single crystals to spherical polycrystals. When the reaction time was prolonged from 6 to 36 h, solid Cu_2O octahedra could be changed to a mixture of hollow Cu_2O octahedra and irregular Cu particles. After removing Cu particles, pure Cu_2O hollow octahedra could be obtained. The formation mechanism of hollow Cu_2O octahedra was discussed. Similarly, hollow Cu_2O spheres could also be obtained using this method. The prepared hollow octahedral Cu_2O particles exhibited a higher photocatalytic activity for photodegradation of *p*-nitrophenol aqueous solution under visible-light illumination than other Cu_2O particles with different morphologies (hollow spheres, solid octahedra, and solid spheres).

1. Introduction

In recent years, there has been increasing interest in the controlled synthesis of inorganic micro- and nanostructures with well-defined shapes and sizes, owing to their widespread potential applications, such as photonics, nanoeletronics, catalysis, information storage, and biosensors.[1−6] As an important p-type semiconductor with a direct band gap of about 2.2 eV, cuprous oxide (Cu_2O) is a promising material with potential applications in solar energy conversion,[7] electrode materials in lithium ion batteries,[8] sensing,[9] and photocatalytic degradation of organic pollutants.[10] In the past decade, many efforts have been developed to prepare Cu_2O micro- and nanocrystals with various morphologies, such as nanospheres,[9] wires,[11,12] rods,[13] cubes,[14] multipod branches,[15] pyramids,[16] octahedra,[17−20] and hollow structures.[21−28]

Compared to solid particles, hollow structures often exhibit unique features including being lightweight, because of central hollow voids, and having large specific surface areas, owing to the presence of both interior and exterior surfaces.[29−33] In recent years, various Cu_2O hollow structures have been prepared by different methods. There have been two main preparative routes for the synthesis of hollow Cu_2O. In the template method, various templates have been used to synthesize Cu_2O, such as PEG,[21] CTAB,[22] and gelatin.[23] Another preparative strategy to synthesize hollow Cu_2O was based on the Ostwald ripening mechanism.[24−27] Although many efforts have been devoted to synthesizing hollow Cu_2O, the hollow structures obtained are mostly spherical, polycrystalline shells consisting of primary particles. Recently, Qi and co-workers reported the one-pot synthesis of octahedral Cu_2O nanocages via a catalytic solution route.[28] Zeng et al. reported the preparation of hollow nanocubes of Cu_2O via reductive self-assembly of CuO nanocrystals.[25] However, it remains a great challenge to develop a feasible method for the synthesis of hollow Cu_2O structures with nonspherical morphologies.

*Corresponding author. Phone: +86-10-82627058. Fax: +86-10-62561822. E-mail: flyuan@home.ipe.ac.cn.

It is well-known that the copper-citrate complex (Benedict's solution) can be reduced by glucose to form Cu_2O, which is widely used in the analytical determination of saccharides.[34] Herein, we report the synthesis of octahedral Cu_2O particles using this method through adjusting reaction conditions, which is a more simple method to synthesize Cu_2O octahedra compared to others.[17−20] More importantly, the hollow structure of Cu_2O octahedra can be obtained by adjusting reaction conditions. A possible formation mechanism was proposed to account for the production of hollow structures. The effects of reaction conditions such as glucose concentration, reaction time, and reaction temperature on morphology of Cu_2O particles were investigated. The adsorption ability and photocatalytic activity of the samples were evaluated by the phtocatalytic degradation of *p*-nitrophenol aqueous solution under visible-light illumination.

2. Experimental Section

2.1. Preparation. All the chemicals were analytical grade reagents used without further purification. In a typical preparation, $CuSO_4 \cdot 5H_2O$ was dissolved in 60 mL of deionized water to prepare the precursor solution with the concentration 0.04 M. Then ammonium citrate (0.4 g) and anhydrous sodium carbonate (0.4 g) were added to the copper sulfate solution under constant stirring. After the solution was stirred for 10 min, glucose (0.6−1.6 M) was added to the above solution, with constant stirring for another 10 min. Next, the above solution was transferred into a 100 mL Teflon-lined stainless steel autoclave, followed by a hydrothermal treatment at 95 to 150 °C for 6−36 h. After the reaction, the powder samples were sonicated, filtered, washed with distilled water and ethanol, and dried at 30 °C for 4 h.

2.2. Characterization. The crystalline phase of the samples was characterized by X-ray diffraction (XRD, X'pert PRO, Panalytical, Cu Kα radiation) in a 2θ range from 20° to 80°. Their size and morphology were inspected with field scanning electron microscopy (FESEM, JEOL JSM-6700F) and transmission electron microscopy (TEM, H-800).

2.3. Measurement of Photocatalytic Activity. The photodegradation of *p*-nitrophenol under visible-light irradiation was selected to study the photocatalytic activity of these Cu_2O particles. A 0.1 g sample of Cu_2O particles with different morphologies was

 Published on Web 11/24/2009

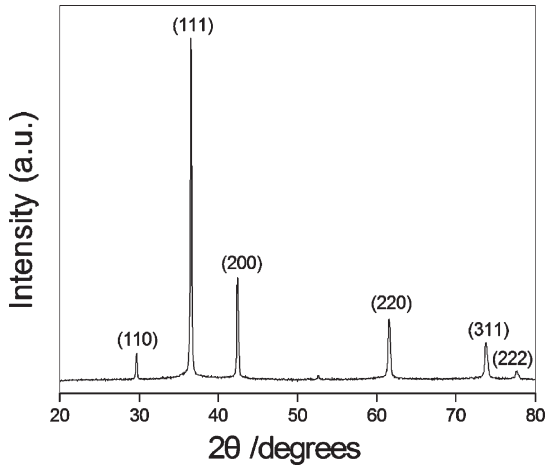

Figure 1. XRD pattern of Cu_2O octahedra obtained with 0.6 M glucose at 95 °C for 6 h.

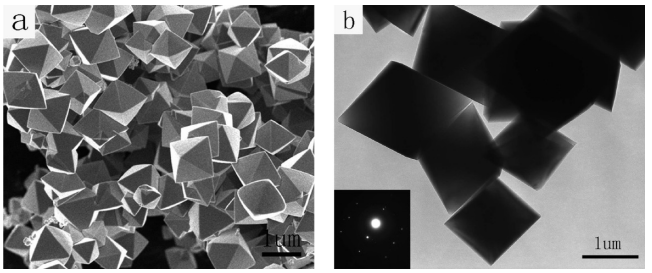

Figure 2. (a) SEM image of the octahedral Cu_2O crystals; (b) TEM image of the octahedral Cu_2O crystals (inset is the corresponding SAED pattern).

dispersed in a 50 mL *p*-nitrophenol aqueous solution (25 mg L^{-1}). The photocatalytic reactions were carried out at room temperature, using a 100 W daylight lamp as light source. The concentration of *p*-nitrophenol was analyzed through a UV−vis spectrophotometer (Unico Uv-2102 PC).

3. Results and Discussion

3.1. Formation of the Cu_2O Octahedra. Figure 1 displays a typical XRD pattern of the product prepared with 0.04 M $Cu(SO_4)_2 \cdot 5H_2O$ and 0.6 M glucose at 95 °C for 6 h. All diffraction peaks can be indexed to the cubic phase of Cu_2O crystals (JCPDS File No. 05-0667). No peaks of impurity are detected in the XRD pattern, indicating the formation of pure Cu_2O under these experimental conditions.

Figure 2a shows an SEM image of the cuprous oxide particles synthesized with 0.04 M $Cu(SO_4)_2 \cdot 5H_2O$ and 0.6 M glucose at 95 °C for 6 h. It reveals that the sample is a regular octahedron with a narrow size distribution, and the edge size of these octahedrons is about 1 μm. A TEM image of the octahedra is shown in Figure 2b. The TEM image in Figure 2b shows that the product has a uniform tetragonal projected shape, consistent with the octahedron-like morphology observed by SEM. The corresponding SAED pattern, as shown in the inset of Figure 2b, taken from an individual Cu_2O octahedron, reveals it is a perfect cubic Cu_2O single crystal.

It was found that citrate was a crucial factor in the formation of the octahedral Cu_2O particles. Preliminary experiments demonstrated that only irregular particles were obtained without citrate. In our experiments, citrates

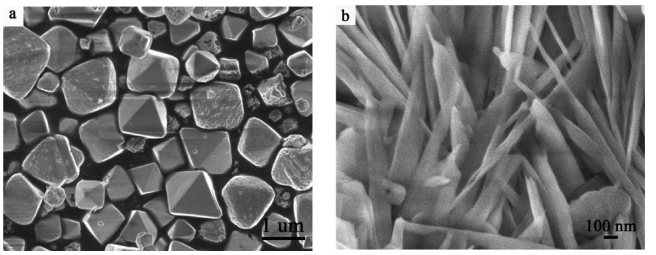

Figure 3. SEM images of Cu_2O particles prepared with different temperatures: (a) 130 °C and (b) 150 °C.

coordinate with Cu^{2+} and form the water-soluble complex of Cu-citrate. Formation of the complex decreased the free Cu^{2+} concentration in solution, which resulted in a relatively slow reaction rate of the reduction of copper-citrate with glucose. Such a slow reaction rate was favorable for the fast growth rate along ⟨100⟩ compared to that along ⟨111⟩ due to the lowest energy of the {111} surfaces of the fcc crystal.[35] It should be mentioned that the octahedral Cu_2O crystals obtained in our experiments were different with the report (also with citrate as structure directing agent),[14] in which not octahedral Cu_2O crystals but cubic Cu_2O crystals were obtained. It may be ascribed to the different pH and reaction temperature of two experiments.

3.2. Effect of Reaction Temperature on Cu_2O Particle Morphology. The reaction temperature played a key role in synthesizing pure and regular octahedral Cu_2O particles. Octahedral Cu_2O particles with a smooth surface (as shown in Figure 2a) can be formed over a range of temperatures from 90 to 110 °C. However, after the reaction temperature was increased to 130 °C, the obtained octahedrons became nonuniform and irregular, as shown in Figure 3a. It was interesting that, when the reaction temperature was further increased to 150 °C, the obtained Cu_2O became ribbon-like (Figure 3b). XRD analysis confirmed the obtained ribbon products were pure Cu_2O. We thought that the increase of reaction temperature might result in different adsorption ability of citrate ions on the different planes of Cu_2O nuclei, which kinetically favor the preferential crystal growth along one dimension direction.[36] The exact formation mechanism of Cu_2O ribbons needs to be further investigated. When the reaction temperature was further increased to 180 °C, no pure Cu_2O but a mixture of Cu_2O and Cu particles was obtained, and some carbonaceous microspheres formed through glucose dehydration.

3.3. Effect of Glucose Concentration on Cu_2O Morphology. The effect of the glucose concentration on the morphology of Cu_2O was investigated under the temperature 95 °C and the reaction time 6 h. Octahedral Cu_2O particles were obtained with glucose concentration 0.6 M as shown in Figures 2a and 4a. When the concentration of glucose was increased to 1.1 M, the {111} surfaces of these octahedrons became arched and the octahedral edge became obsolete (Figure 4b). As the glucose concentration was further increased to 1.6 M, the Cu_2O particles became spheres completely, and no octahedral Cu_2O particles were founded (Figure 4c). Different from the single crystallinity of the octahedral Cu_2O particles, these spherical particles were all polycrystals, as evidenced by the ringlike SAED pattern taken on a single spherical particle (inset of Figure 4c). The shape change of Cu_2O from octahedron to sphere as glucose concentration increased can be explained by the diffusion mechanism[37,38] and the random aggregation mechanism.[39−42] The diffusion

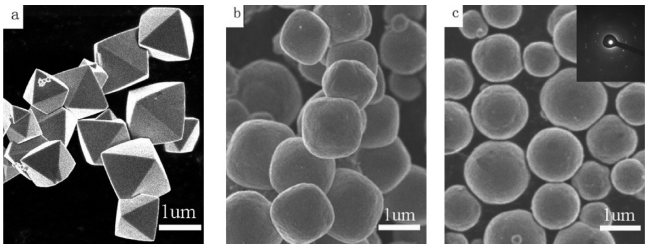

Figure 4. SEM images of Cu_2O particles prepared with different glucose concentrations: (a) 0.6 M; (b) 1.1 M; and (c) 1.6 M (inset is the corresponding SAED pattern).

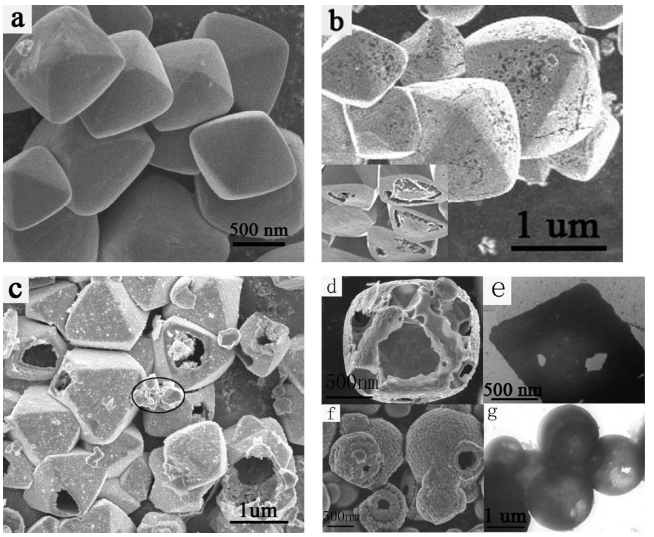

Figure 5. (a−c) SEM images of the sample prepared for different times: (a) 2 h; (b) 24 h; (c) 36 h. (d) SEM image of a single Cu_2O hollow octahedron after removing Cu particles; (e) TEM image of a single Cu_2O hollow octahedron after removing Cu particles; (f) SEM image of hollow Cu_2O spheres after removing Cu particles; (g) TEM image of hollow Cu_2O spheres after removing Cu particles.

mechanism was generally accepted to explain the formation of monodispersed single crystals, while the random aggregation mechanism was employed to explain the formation of monodispersed polycrystals. The results of the present work imply that these two mechanisms could have action on the morphologies of the resultant Cu_2O particles in a competitive way. When the concentration of glucose was low, the nucleation of Cu_2O was followed by diffusion, and octahedral single crystals were obtained. When the concentration of glucose was high, aggregation prevailed, and thus spherical polycrystals were obtained. The rather smooth surface of the spherical polycrystals may be due to the rapid contact recrystallization of the constituent primary particles.

3.4. Effect of Reaction Time on Cu_2O Particle Morphology. The effect of the reaction time on the size and morphology of Cu_2O was investigated under the temperature 95 °C and the glucose concentration 0.6 M. SEM and TEM images of products formed with different reaction times are shown in Figure 5. After the sample was heated for 2 h, octahedral Cu_2O was formed, but the size of these particles was smaller (around 500−800 nm), as shown in Figure 5a. The color of the solution was still green, indicating most of the Cu^{2+} was not reduced at this stage. After being heated for 6 h, the size of the Cu_2O octahedrons was increased to about 1 μm, as shown in Figures 2a and 4a, and all Cu^{2+} have been reduced to Cu_2O at this stage (justified by solution color). XRD

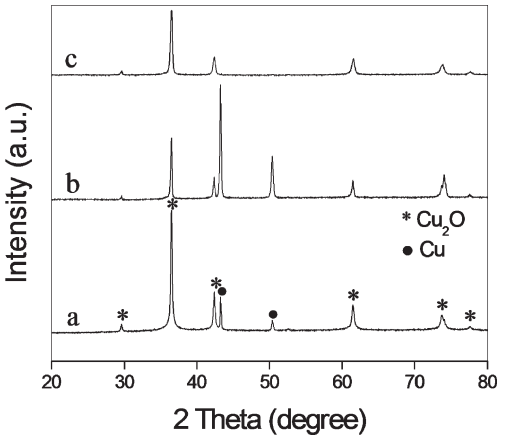

Figure 6. XRD patterns of the sample obtained for different times: (a) 24 h; (b) 36 h. (c) XRD pattern of the sample after removing Cu particles.

analysis confirmed they were pure Cu_2O (Figure 1). After reaction for 24 h, the shape of octahedral particles has no obvious change, but some pinholes appeared on surfaces of these octahedrons, as shown in Figure 5b. Several broken octahedrons obtained at this stage were shown in the inset of Figure 5b, from which we can see the core−shell structure of the sample. In order to show the core−shell structure more clearly, a SEM image of a singe core−shell particle was shown in Figure S1. The corresponding XRD result shows that the diffraction peaks of Cu appeared in addition to the diffraction peaks of Cu_2O, indicating the formation of Cu in these octahedral particles (Figure 6a). When the sample was heated for 36 h, the individual octahedron became hollow and some irregular particles appeared outside the hollow octahedra (Figure 5c). Moreover, the XRD pattern shows that the intensities of the diffraction peaks of Cu increase, whereas that of Cu_2O has an obvious decrease (Figure 6b). After analysis of the SEM image, we speculated that the hollow octahedrons were Cu_2O, while the irregular particles located outside the hollow octahedrons were Cu (as marked out by the ellipse in Figure 5c). The EDS analysis confirmed our speculation (Figure S2). In the EDS spectrum of a typical hollow octahedron, the peaks of O and Cu were obviously observed without any other peaks (Ni peaks appearing in the spectrum are due to background from the nickel TEM grid). In the EDS spectrum of irregular particles, the peak of O was greatly weakened compared to that of hollow octahedron. The existence of trace O in the EDS spectrum of irregular particles may be ascribed to partial oxidation of Cu during TEM sample preparation or the effects of Cu_2O hollow octahedron. Using the method reported in the literature,[43] we successfully removed the Cu phase from Cu_2O particles, and pure hollow Cu_2O octahedrons were obtained. The corresponding XRD result showed that the diffraction peaks of the Cu phase all disappeared, indicating Cu particles were completely removed using this method (Figure 6c). SEM and TEM images of a single hollow Cu_2O octahedron after removing Cu particles were shown in parts d and e, respectively, of Figure 5. Similar to the hollowing process of solid Cu_2O octahedra, when heating time was prolonged to 36 h, the solid Cu_2O spheres can also be transferred to the mixture of hollow Cu_2O spheres and irregular Cu particles. After removing Cu particles, pure Cu_2O hollow spheres can be obtained. SEM and TEM images of pure Cu_2O hollow

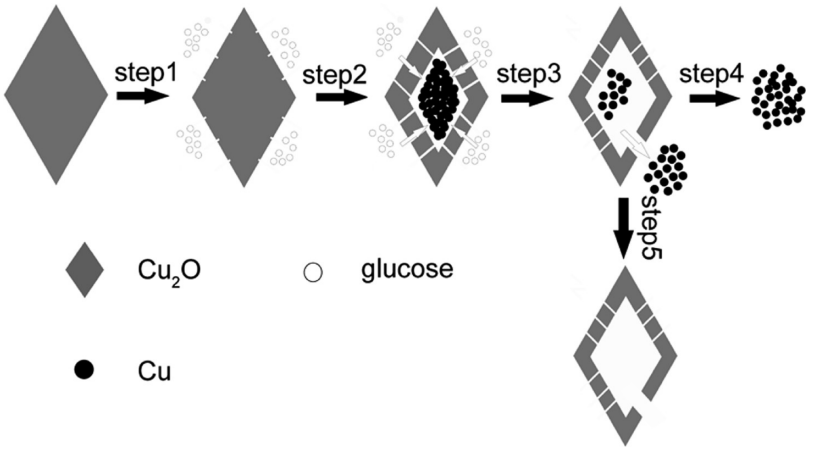

Figure 7. Schematic illustration of the formation of hollow Cu_2O octahedrons: step 1, pinholes appeared on the surface of Cu_2O octahedra; step 2, pinholes went deeper into the interior of the Cu_2O, and glucose diffused to the interior of the Cu_2O through these pinholes and reacted with interior Cu_2O; step 3, octaheda were broken and Cu particles flew out; step 4, when reacted for 60 h, hollow Cu_2O octahedra were reduce to Cu completely; step 5, pure Cu_2O hollow octahedrons were obtained after removing Cu particles.

spheres were shown in parts f and g, respectively, of Figure 5. It should be noted that, in either hollow octahedral or spherical Cu_2O particles, a hole appeared on their surface.

3.5. Morphology−Evolution Mechanism of Cu_2O from Octahedra to Hollow Structures. From the above experiments and analysis, a possible formation mechanism of hollow Cu_2O octahedra was proposed, and a scheme was summarized in Figure 7. Octahedral Cu_2O particles were precipitated out first due to the hydrothermal condition under the assistance of citrate. When all Cu^{2+} in the solution have been reduced to Cu_2O, the Cu_2O can be further reduced to Cu, as plenty of glucose existed in the solution. In the early stage, the reduction of Cu_2O randomly located on their surface, and pinholes randomly formed on the surface of Cu_2O octahedra. Once the pinholes were formed on the surface of Cu_2O octahedra, further reduction of Cu_2O would occur preferentially inside the pinholes, since the energy of the pinholes' interior is higher than that of the Cu_2O surface. The proposed higher energy of the pinholes' interior compared to that of the Cu_2O surface is explained by the fact that the inner part of Cu_2O was reduced to Cu prior to outside Cu_2O. It can also be understood that, in order to reduce surface energy, the surface of Cu_2O octahedra may go through surface reconstruction or adsorption, but the newly formed surface of the pinholes' interior have not enough time for reconstruction before being reduced. So the newly formed surface of the pinholes interior was more easily reduced than the outside surface of Cu_2O octahedra. With aging, the hole on the surface became bigger and bigger, and the inner part of Cu_2O was gradually reduced to Cu, and a core−shell structure was formed. When reacted for 36 h, as has been shown in Figure 5c, a big hole appeared on the surface of the hollow Cu_2O octahedra. The formation of the big hole on the surface of hollow Cu_2O octahedra may be caused by the local reduction of the Cu_2O shell at either step 2 or step 3. Another possible reason for the formation of the big hole on the surface of Cu_2O octahedra was the outward diffusion of Cu, which was caused by the concentration gradient of Cu. After the big hole was formed, Cu particles could flow out from the hole to the solution (step 3). After removing the Cu phase, pure Cu_2O hollow octahedra with a hole on their surface were obtained (step 5). In our experiments, the formation of pinholes on the surface of Cu_2O octahedra caused the prior reduction of the Cu_2O interior. Thus, octahedral Cu_2O shells were preserved and not reduced to Cu when reacted for 36 h. However, when the reaction time was further prolonged (reacted for 60 h), the hollow Cu_2O octahedra could also be reduced to irregular Cu particles (step 4). Thus, proper reaction time was important for the formation of hollow octahedra.

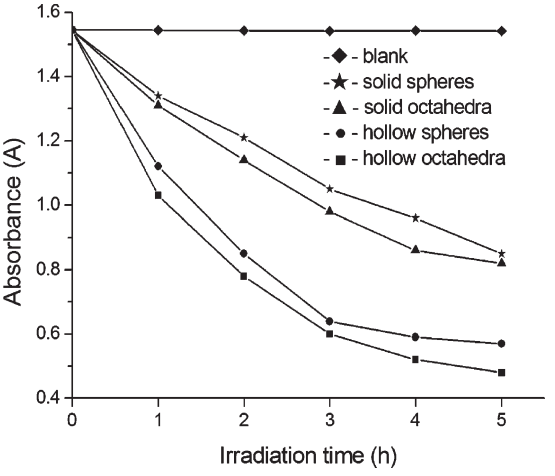

Figure 8. Plots of absorbance (A) vs irradiation time (t) for the Cu_2O particles with different morphologies.

3.6. Photocatalytic Activity of Cu_2O Particles. In recent years, Cu_2O has been used as a photocatalyst for the hydrogen production and organic pollutants degradation under visible light.[18,44] To demonstrate the potential applicability of the present Cu_2O related to its morphology, the adsorption ability and photocatalytic activity of Cu_2O particles with different morphologies (octahedra, spheres, hollow octahedra, hollow spheres) were compared to study the morphology-dependent photocatalytic property. The degradation of *p*-nitrophenol was selected as a reference, and the characteristic absorption of *p*-nitrophenol at 320 nm was selected for monitoring the adsorption and photocalytic degradation process. Figure 8 shows the comparison of photocatalytic activities of different samples. The blank test indicates that, in the absence of Cu_2O, *p*-nitrophenol shows no photodegradation under visible-light irradiation. It can be seen that, in the presence of hollow Cu_2O octahedrons, the

concentration of *p*-nitrophenol shows a faster decrease. When irradiated for 5 h, the degradation rate of *p*-nitrophenol is up to 68%. The adsorption ability and photocatalytic activity of hollow octahedral Cu_2O particles is much higher than those of solid octahedral Cu_2O particles. Similar to it, the adsorption ability and photocatalytic activity of hollow Cu_2O spheres are also higher than those of solid Cu_2O spheres. The higher adsorption and photocatalytic activity of hollow Cu_2O particles may be ascribed to their higher surface areas compared to solid particles. It should be noted that, whether solid or hollow particles, the adsorption ability and photocatalytic activity of Cu_2O octahedrons are higher than those of Cu_2O spheres. The improvement in photocatalytic ability of octahedral Cu_2O may be ascribed to the exposed {111} surfaces. This finding further implies that adsorption ability and photocatalytic activity are related to its morphology and structure.

4. Conclusion

In summary, we demonstrated a new method for the synthesis of octahedral Cu_2O single crystals through reducing copper-citrate with glucose. The effects of glucose concentration, reaction temperature, and time on the morphology and structure of Cu_2O were investigated. The increase of the glucose concentration induced a morphology change of Cu_2O from octahedral single crystals to spherical polycrystals. Increasing of reaction time induced solid octahedral and spherical Cu_2O transform to the mixture of hollow Cu_2O octahedra and irregular Cu particles. The formation mechanism of hollow Cu_2O structure was discussed. Pure hollow Cu_2O octahedra and spheres can be obtained after removing Cu particles. Photocatalytic experiments show that hollow octahedral Cu_2O particles exhibit a higher photocatalytic activity for the photodegradation of *p*-nitrophenol under visible-light illumination than other Cu_2O particles with different morphologies (hollow spheres, solid octahedra, and solid spheres).

Acknowledgment. This work was supported by National Natural Science Foundation of China (No. 50907072).

Supporting Information Available: SEM image of a core−shell structure particle when reacted for 24 h and EDS spectrum of a hollow octahedron (a) and irregular particles (b), which reacted for 36 h with glucose concentration 0.6 M. This material is available free of charge via the Internet at http://pubs.acs.org.

References

(1) Jiang, P.; Bertone, J. F.; Colvin, V. L. *Science* **2001**, *291*, 453–457.
(2) Punters, V. F.; Krishnan, K. M.; Alivisatos, A. P. *Science* **2001**, *291*, 2115–2117.
(3) Huang, Y.; Duan, X.; Cui, Y.; Lauhon, L.; Kim, K. H.; Lieber, C. M. *Science* **2001**, *294*, 1313–1317.
(4) Yin, S.; Sato, T. *Ind. Eng. Chem. Res.* **2000**, *39*, 4526–4530.
(5) Wang, X.; Yu, L. J.; Hu, P.; Yuan, F. L. *Cryst. Growth Des.* **2007**, *7*, 2415–2418.
(6) Murphy, C. J.; Jana, N. R. *Adv. Mater.* **2002**, *14*, 80–82.
(7) Briskman, R. N. *Sol. Energy Mater. Sol. Cells* **1992**, *27*, 361–368.
(8) Laik, B.; Poizot, P.; Tarasscon, J. M. *J. Electrochem. Soc.* **2002**, *149*, A251–255.
(9) Zhang, J.; Liu, J.; Peng, Q.; Wang, X.; Li, Y. *Chem. Mater.* **2006**, *18*, 867–871.
(10) Ramirez-Ortiz, J.; Ogura, T.; Medina-Valtierra, J.; Acosta-Ortiz, S. E.; Bosch, P.; Delos Reyes, J. A.; Lara, V. H. *Appl. Surf. Sci.* **2001**, *174*, 177–184.
(11) Wang, W. Z.; Wang, G. H.; Wang, X. S.; Zhan, Y. J.; Liu, Y. K.; Zheng, C. L. *Adv. Mater.* **2002**, *14*, 67–69.
(12) Xiong, Y.; Li, Z.; Zhang, R.; Xie, Y.; Yang, J.; Wu, C. Z. *J. Phys. Chem. B* **2003**, *107*, 3697–3702.
(13) Yao, W. T.; Yu, S. H.; Zhou, Y.; Jiang, J.; Wu, Q. S.; Zhang, L.; Jiang, J. *J. Phys. Chem. B* **2005**, *109*, 14011–14016.
(14) Wang, D. B.; Mo, M. S.; Yu, D. B.; Li, L. Q.; Qian, Y. T. *Cryst. Growth Des.* **2003**, *3*, 717–720.
(15) Xu, J. S.; Xue, D. F. *Acta Mater.* **2007**, *55*, 2397–2406.
(16) Liu, R.; Oba, F.; Bohannan, E. W.; Ernst, F.; Switzer, J. A. *Chem. Mater.* **2003**, *15*, 4882–4885.
(17) Song, H. C.; Cho, Y. S.; Huh, Y. D. *Mater. Lett.* **2008**, *62*, 1734–1736.
(18) Ng, C. H. B.; Fan, W. Y. *J. Phys. Chem. B* **2006**, *110*, 20801–20807.
(19) He, P.; Shen, X.; Gao, H. *J. Colloid Interface Sci.* **2005**, *284*, 510–515.
(20) Xu, H. L.; Wang, W. Z.; Zhu, W. *J. Phys. Chem. B* **2006**, *110*, 13829–13834.
(21) Xu, Y. Y.; Chen, D. R.; Jiao, X. L.; Xue, K. Y. *J. Phys. Chem. C* **2007**, *111*, 16284–16289.
(22) Xu, H. L.; Wang, W. Z. *Angew. Chem., Int. Ed.* **2007**, *46*, 1489–1492.
(23) Xu, L. S.; Chen, X. H.; Wu, Y. R.; Chen, C. S.; Li, W. H.; Pan, W. Y.; Wang, Y. G. *Nanotechnology* **2006**, *17*, 1501–1505.
(24) Chang, Y.; Teo, J. J.; Zeng, H. C. *Langmuir* **2005**, *21*, 1074–1079.
(25) Teo, J. J.; Chang, Y.; Zeng, H. C. *Langmuir* **2006**, *22*, 7369–7377.
(26) Zhang, H. G.; Zhu, Q. S.; Zhang, Y.; Wang, Y.; Zhao, L.; Yu, B. *Adv. Funct. Mater.* **2007**, *17*, 2766–2771.
(27) Zhu, H. T.; Wang, J. X.; Xu, G. Y. *Cryst. Growth Des.* **2009**, *9*, 633–638.
(28) Lu, C. H.; Qi, L. M.; Yang, J. H.; Wang, X. Y.; Zhang, D. Y.; Xie, J. L.; Ma, J. M. *Adv. Mater.* **2005**, *17*, 2562–2567.
(29) Wang, X.; Fu, H. B.; Peng, A. D.; Zhai, T. Y.; Ma, Y.; Yuan, F. L.; Yao, J. N. *Adv. Mater.* **2009**, *21*, 1–5.
(30) Chen, F. Y.; Ma, H.; Li, Y. M.; Chen, J. *Inorg. Chem.* **2007**, *46*, 788–794.
(31) Chen, J. Y.; Wiley, B.; Li, Z. Y.; Campbell, D.; Saeki, F.; Cang, H.; Au, L.; Lee, J.; Li, X. D.; Xia, Y. N. *Adv. Mater.* **2005**, *17*, 2255–2261.
(32) Yan, C. L.; Xue, D. F. *J. Phys. Chem. B* **2006**, *110*, 7102–7106.
(33) Yan, C. L.; Liu, J.; Liu, F.; Wu, J. S.; Gao, K.; Xue, D. F. *Nanoscale Res. Lett.* **2008**, *3*, 473–480.
(34) Petrucci, R. H. *General Chemistry*, 4th ed.; Macmillan Publishing Company: New York, 1985; p 848.
(35) Wang, Z. L. *J. Phys. Chem. B* **2000**, *104*, 1153–1175.
(36) Wang, N.; Cai, Y.; Zhang, R. Q. *Mater. Sci. Eng. Res.* **2008**, *60*, 1–51.
(37) Lamer, V. K.; Dinegar, R. H. *J. Am. Chem. Soc.* **1950**, *72*, 4847–4854.
(38) Lamer, V. K. *Ind. Eng. Chem.* **1952**, *44*, 1270–1277.
(39) Hsu, W. P.; Ronnquist, L.; Matijevic, E. *Langmuir* **1988**, *4*, 38–44.
(40) Ocana, M.; Rodriguez-Clemente, R.; Serna, C. J. *Adv. Mater.* **1995**, *7*, 212–216.
(41) Lee, S. H.; Her, Y. S.; Matijevic, E. *J. Colloid Interface Sci.* **1997**, *186*, 193–202.
(42) Privman, V.; Goia, D. V.; Park, J.; Matijevic, E. *J. Colloid Interface Sci.* **1999**, *213*, 36.
(43) Wang, Z. Y.; Liu, Y.; Zang, M. W.; Kang, Z. J.; Gao, Z. Z. *Anal. Lab.* (*China*) **2001**, *20*, 61–63.
(44) Michikazu, H.; Takeshi, K.; Mutsuko, K.; Sigeru, I.; Junko, K. N.; Kazunari, D.; Kiyoaki, S.; Akira, T. *Chem. Commun.* **1998**, 357–358.